

New Dyes Based on Amino-Substituted Acridizinium Salts—Synthesis and Exceptional Photochemical Properties

Heiko Ihmels,* Bernd Engels, Katja Faulhaber, and Christian Lennartz^[a]

Abstract: The novel amino-substituted acridizinium salts **5a** and **5b** represent a new class of cyanine dyes which exhibit intense color along with efficient fluorescence properties. These dyes show moderate solvatochromism in their absorption and emission spectra. The absorption and emission shifts of the two chromophores display a reasonable correlation with solvent parameters such as

donor and acceptor number. It was found that the dyes **5a** and **5b** interact with DNA, with quenching of the band intensities accompanied with a red shift of the absorption and emission bands.

Keywords: acridizinium salts • dyes • fluorescence • NMR spectroscopy • photochemistry

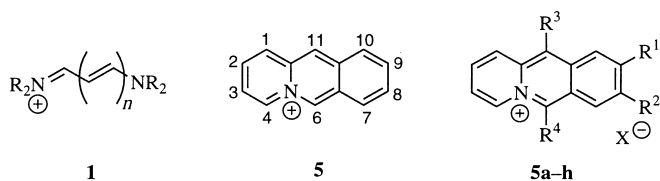
Moreover, irradiation of salts **5a** and **5b** in the presence of DNA results in DNA damage. Solution photolysis of acridizinium salt **5a** gave the head-to-tail dimers as the major products (> 95%), whereas the acridizinium salt **5b** afforded the *anti*-head-to-tail dimer along with both head-to-head isomers. The latter are thermally labile and rapidly revert to the monomer.

Introduction

Cyanine dyes of the general polymethine structure **1** are among the most versatile functional dyes.^[1] Besides their use as colorants,^[2] they have considerable potential for application in energy conversion^[3] as laser dyes,^[4] and as optoelectronic and photonic devices.^[5] Moreover, some cyanine and related dyes show strong interactions with nucleic acids with efficient intercalation and photodamage of DNA.^[6] Although most polymethine dyes exhibit efficient absorption over a remarkably long range of the optical spectrum,^[1] the number of highly fluorescent dyes is rather small; this is mainly a result of radiationless deactivation of excited states by photochemical isomerization or by conformational changes in the dye molecules.^[1b] Thus, the application of these compounds as potential fluorescence sensors^[7] or as electro-, chemo-, and photoluminescent devices^[8] is limited. In order to achieve satisfactory fluorescent properties of cyanine compounds, we wished to design new molecules in which the structural feature of a cyanine dye is incorporated within the rigid framework of anthracene,^[9] a highly fluorescent chromophore. The 9-aminoacridizinium salt (**5a**) (Figure 1) was chosen as a novel cyanine dye with both intense color and the propensity for efficient emission properties.

We report the synthesis of the novel acridizinium salt **5a** along with its photophysical and photochemical properties.^[10]

[a] Dr. H. Ihmels, Prof. Dr. B. Engels, K. Faulhaber, Dipl.-Chem. C. Lennartz
Institut für Organische Chemie, Universität Würzburg
Am Hubland, 97074 Würzburg (Germany)
Fax: (+49) 931-888-4606
E-mail: ihmels@chemie.uni-wuerzburg.de



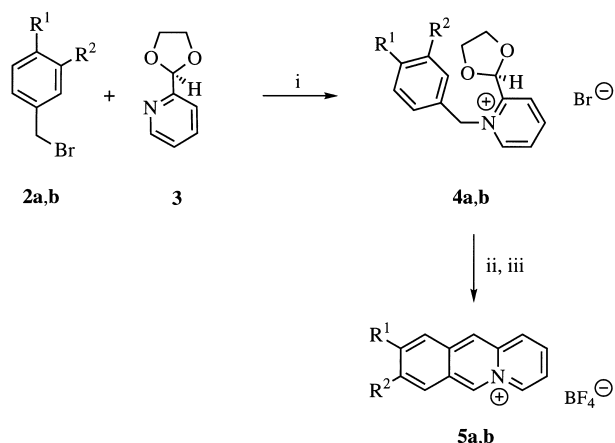
5a: R¹ = NH₂, R² = R³ = R⁴ = H; **5e:** R¹ = R² = R³ = R⁴ = H;
5b: R² = NH₂, R¹ = R³ = R⁴ = H; **5f:** R¹ = Br, R² = R³ = R⁴ = H;
5c: R¹ = phthalimidyl, R² = R³ = R⁴ = H; **5g:** R³ = NH₂, R¹ = R² = R⁴ = H;
5d: R² = phthalimidyl, R¹ = R³ = R⁴ = H; **5h:** R⁴ = NH₂, R¹ = R² = R³ = H.

Figure 1. Structures of cyanine dyes **1** and acridizinium salts **5**.

The potential use of this new dye as a fluorescence probe, and as an intercalating and DNA-damaging chromophore was examined. To study the effect of π conjugation on the photophysical and photochemical properties of amino-substituted acridizinium salts, we also investigated the isomeric 8-aminoacridizinium salt (**5b**), which does not exhibit a π -conjugated connection of the quaternary nitrogen atom and the amino group present in cyanine dyes such as **1**.

Results

Synthesis: Acridizinium salts **5a** and **5b** were synthesized by the cyclodehydration method of Bradsher et al. (Scheme 1).^[11] Thus, the pyridine derivative **3** was quaternized with the bromomethylarylphthalimides **2a** and **2b** to give the corresponding pyridinium salts **4a** and **4b** in moderate yields. Treatment of these salts with polyphosphoric acid gave the



2a, 4a: $R^1 = \text{phthalimidyl}, R^2 = \text{H}$; **2b, 4b:** $R^2 = \text{phthalimidyl}, R^1 = \text{H}$;
5a: $R^1 = \text{NH}_2, R^2 = \text{H}$; **5b:** $R^2 = \text{NH}_2, R^1 = \text{H}$

Scheme 1. Synthesis of acridizinium salts **5a** and **5b**; i) DMSO, RT, 7 d; ii) polyphosphoric acid (84%), 90°C, 16 h; iii) HBF_4 (50%).

amino-substituted acridizinium salts **5a** and **5b** in 45% and 37% yields, along with trace amounts of the phthalimidyl-substituted acridizinium salts **5c** and **5d**. These byproducts could also be transformed quantitatively to the free amines by treatment with sodium sulfide in aqueous DMSO.^[12] The amine **5a** is only weakly basic and may be obtained as the free amine even from acidic solutions, whereas isomer **5b** is more basic, and the reaction mixture requires neutralization in order to isolate the non-protonated form. In the case of amine **5b**, analysis of the initially isolated product by ^1H NMR spectroscopy showed small amounts (ca. 5%) of another byproduct, which had substantial overlap with the signals of product **5b**. Accordingly, we assume that the 10-amino-substituted isomer was formed in minor amounts. This assumption is based on the characteristic ^1H NMR signal of the 6-H proton ($\delta = 10.30$) and a doublet at $\delta = 7.20$ with a coupling constant of 9 Hz, which may correspond to the 7-H proton (for comparison, the singlet of 7-H in **5b** is located at $\delta = 7.12$). This byproduct was readily removed by two recrystallizations from methanol. The structures of the acridizinium salts **5a–5d** were confirmed by ^1H and ^{13}C NMR spectroscopy, mass-spectrometric data, and elemental analyses.

Spectroscopic data: The acridizinium salt **5a** is an orange or red solid, depending on the solvent chosen for crystallization. The solid isomer **5b** exhibits a deep-red color. In contrast to the parent compound **5e**, which is pale yellow in concentrated solutions and almost colorless in dilute solution, the amino-substituted dyes **5a** and **5b** are red in concentrated solutions.^[13] However, dilute methanolic solutions ($< 10^{-4}\text{M}$) of acridizinium salt **5a** possess a bright green fluorescence, whereas dilute methanolic solutions of dye **5b** are yellow. The long-wavelength region of the UV spectrum of compound **5a** in methanol exhibits a broad band structure with a maximum at $\lambda = 392\text{ nm}$ partially overlapped by a less intense, very broad band ($\lambda = 450\text{ nm}$); the latter is not observed with the parent acridizinium salt **5e**.^[14] The onset of absorption is

around 500 nm. Moreover, the salt **5a** exhibits solvatochromism, that is, the maximum of the p band (S_0-S_1 transition) shifts from $\lambda = 385\text{ nm}$ in water to $\lambda = 397\text{ nm}$ in 1-butanol (Table 1). The UV spectrum in trifluoroacetic acid solution resembles that of the parent compound with three resolved bands at $\lambda = 354, 373,$ and 392 nm . Presumably, the amino group is protonated by the strong acid, thus suppressing the donor–acceptor interaction. The absorption spectrum of dye **5b** is also solvent dependent and exhibits the same features as compound **5a**. However, the maximum of the p band is slightly blue shifted relative to salt **5a** with the onset of absorption located at a higher wavelength, that is, 540 nm. The absorption band maxima of the p band of salt **5b** ranges from 369 nm in water to 389 nm in 2-propanol.

Table 1. Absorption and emission maxima of the acridizinium tetrafluoroborates **5a** and **5b** (in nm, solvents in order of decreasing $E_T(30)$ value)

Solvent	λ_{abs} (5a) ^[a]	$\log \epsilon$ (5a)	λ_{em} (5a) ^[b] (ϕ_{em})	λ_{abs} (5b) ^[a]	$\log \epsilon$ (5b)	λ_{em} (5b) ^[b] (ϕ_{em})
H_2O	385	4.24	507 (0.12)	369	4.04	551 (0.02)
$\text{H}_2\text{O}/\text{DNA}^{\text{[c]}}$	399	3.97	512 (0.07)	392	3.78	558 (0.01)
MeOH	392	4.28	508 (0.18)	383	4.13	557 (0.02)
EtOH	395	4.28	506	388	4.11	559
$\text{CH}_3\text{CO}_2\text{H}$	388	3.79	497 (0.72)	376	4.08	535 (0.04)
1-BuOH	397	4.28		389	4.10	561
2-PrOH	396	4.29	508	389	4.09	559
CH_3CN	386	4.26	501	378	4.10	549
	391	4.26				(0.03)
DMSO	395	4.30	516 (0.10)	386	4.11	563 (0.01)
DMF	394	4.29	512	386	4.13	560
Pyridine	398	4.29	516 (0.13)	388	4.06	564
THF	392	4.08	512 (0.21)	383	3.96	560 (0.04)

[a] $c = 10^{-4}\text{ M}$, S_0-S_1 transition. [b] $\lambda_{\text{ex}} = 380\text{ nm}$; $c = 10^{-5}\text{ M}$, $V = 2\text{ mL}$. [c] $c_{\text{DNA}} = 1\text{ mg mL}^{-1}$.

Acridizinium salt **5a** shows an intense fluorescence maximum around $\lambda = 510\text{ nm}$ along with a weak, broad emission at about $\lambda = 440\text{ nm}$. The latter was not observed in all solvents examined. The wavelength of the emission maximum is also solvent dependent and ranges from $\lambda = 497\text{ nm}$ in acetic acid to $\lambda = 516\text{ nm}$ in pyridine and DMSO (Figure 2, Table 1). In more concentrated solutions (10^{-2} M), the fluorescence intensity decreases and a red shift of the emission maximum was observed along with quenching of the fluorescence intensity. The fluorescence quantum yield was determined to be 0.19 in water and 0.20 in methanol (10^{-5} M). In acetic acid, an exceptionally high quantum yield of 0.72 was found. Preliminary results have shown that the fluorescence has a remarkably long lifetime of $\tau_{\text{Fl}} = 14\text{ ns}$ in water and $\tau_{\text{Fl}} = 16\text{ ns}$ in acetonitrile.^[15] It was also observed that a short-lived fluorescence ($\tau_{\text{Fl}} = 4\text{ ns}$) contributes to a small degree (ca. 5%) to the overall emission. The fluorescence of dye **5a** is remarkably red shifted in the solid state. Thus, a solid sample of 9-aminoacridizinium perchlorate, recrystallized from methanol, emits at $\lambda = 570\text{ nm}$. With tetrafluoroborate as counterion, a solid sample (crystallized from methanol) also exhib-

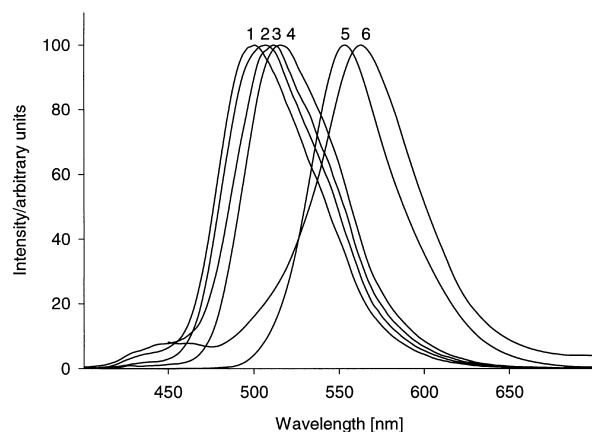


Figure 2. Normalized fluorescence spectra of acridizinium salt **5a** in selected solvents. 1: CH₃CN, 2: H₂O, 3: THF; 4: DMSO, 5: CH₃CN (saturated), 6: solid state.

ited one emission band at $\lambda = 563$ nm (Figure 2). Further experiments with time-delayed recording revealed that these emissions are not phosphorescence.

The 8-aminoacridizinium salt **5b** also exhibits a solvent-dependent emission that is significantly shifted to longer wavelength relative to the dye **5a** (Table 1, Figure 3). Along with a very weak emission at about $\lambda = 440$ nm, a strong

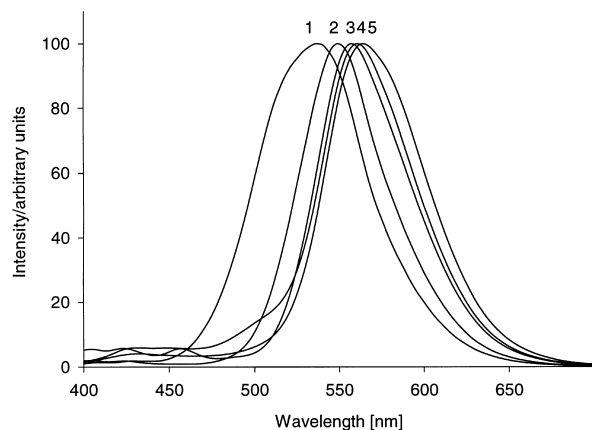


Figure 3. Normalized fluorescence spectra of acridizinium salt **5b** in selected solvents. 1: CH₃COOH, 2: CH₃CN, 3: MeOH; 4: 1-butanol, 5: pyridine.

fluorescence band at $\lambda = 557$ nm was observed in methanol. In polar, aprotic solvents such as DMSO and DMF the weak, broad emission at $\lambda = 440$ nm increased, whilst the initial fluorescence at $\lambda = 560$ nm decreased when the sample was allowed to stand at room temperature. Such behavior was not observed in alcoholic solvents. In acetic acid, the initially recorded fluorescence spectrum exhibited a signal at $\lambda = 535$ nm; however, on standing at room temperature, the emission spectrum changed and displayed a band shift and structure which resembles that of the parent compound **5e**, presumably due to slow protonation of the amino functionality. The fluorescence quantum yield was determined to be $\phi_{\text{Fl}} = 0.02$ in water and methanol—much smaller than the quantum yield for the isomer **5a**. The fluorescence lifetime in

water is $\tau_{\text{Fl}} = 11$ ns. Acridizinium salt **5b** exhibits almost no emission in the solid state.

Interaction with DNA: The amino-substituted acridizinium salts **5a** and **5b** were titrated with *calf thymus* DNA (1 mg mL⁻¹) in aqueous solution, and the addition monitored by UV and fluorescence spectroscopy (Figures 4–7). For

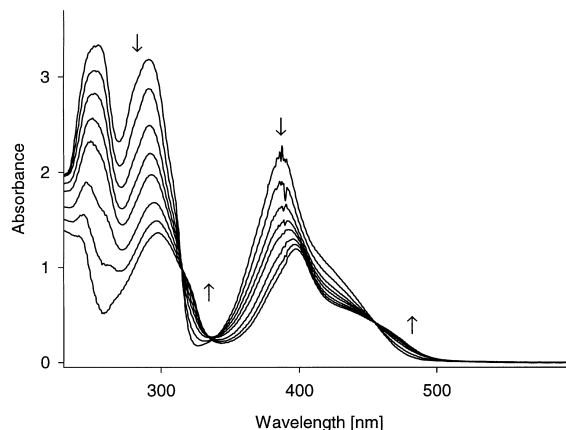


Figure 4. UV-monitored titration of acridizinium salt **5a** with *calf thymus* DNA in water.

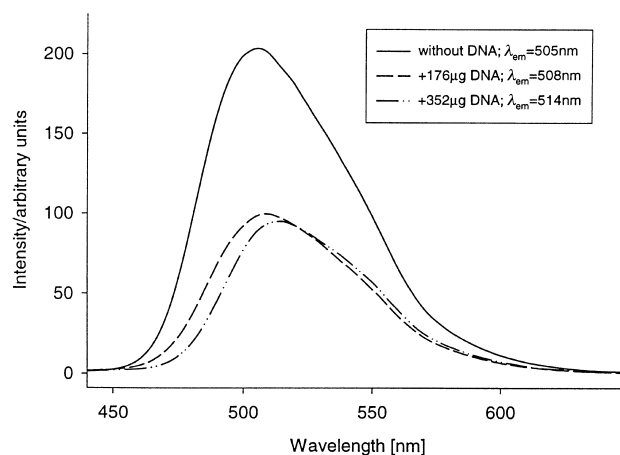


Figure 5. Fluorescence-monitored titration of acridizinium salt **5a** with *calf thymus* DNA in water.

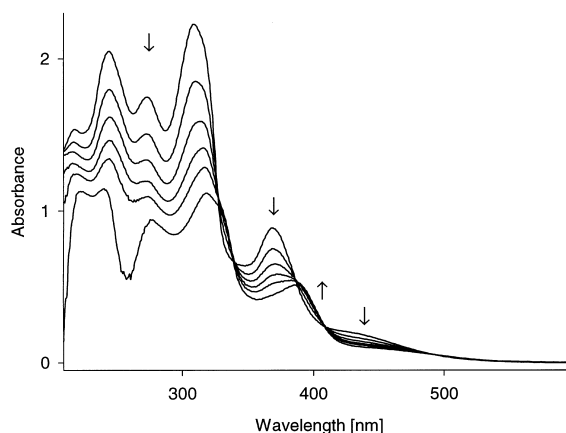


Figure 6. UV-monitored titration of acridizinium salt **5b** with *calf thymus* DNA in water.

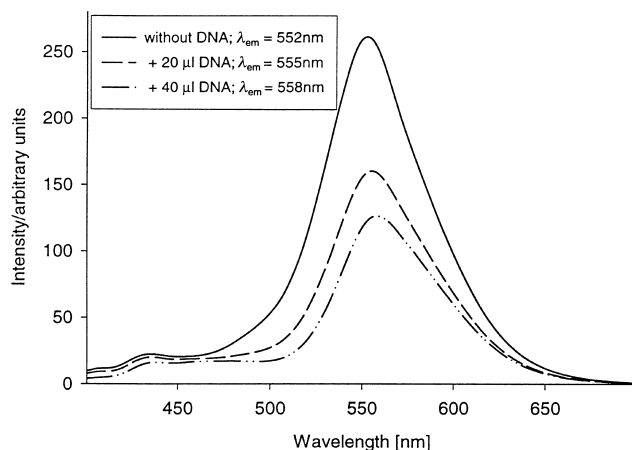


Figure 7. Fluorescence-monitored titration of acridizinium salt **5b** with *calf thymus* DNA in water.

comparison, the parent compound **5e** was titrated with DNA under identical conditions (Figures 8 and 9). In each case, the absorbance of the chromophores decreased significantly on successive addition of the DNA solution and an isobestic point was observed. However, whereas the unsubstituted

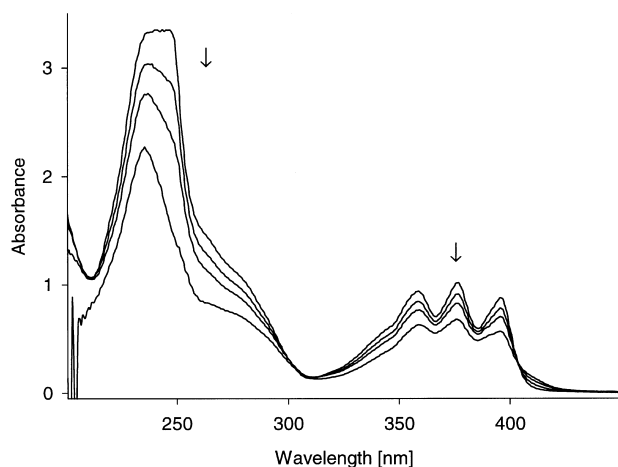


Figure 8. UV-monitored titration of acridizinium salt **5e** with *calf thymus* DNA in water.

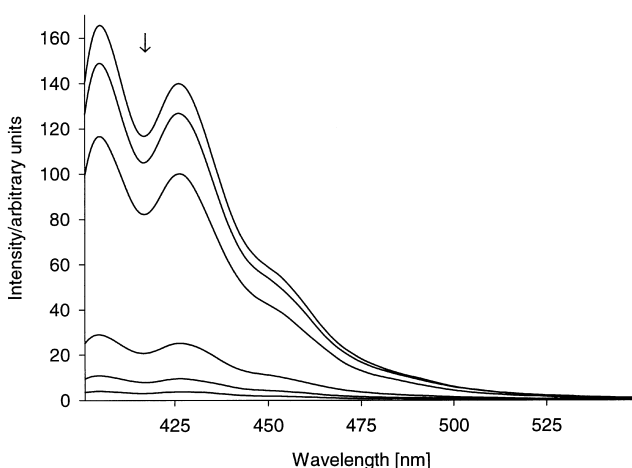


Figure 9. Fluorescence-monitored titration of acridizinium salt **5e** with *calf thymus* DNA in water.

arene **5e** showed only a slight absorption tail in the long-wavelength region (presumably due to line broadening) and the absorption band shifts were unchanged, a significant bathochromic shift was observed on DNA addition to both the aminoacridizinium salts **5a** and **5b**. Moreover, the fluorescence band intensity of all three salts **5a**, **5b**, and **5e** was significantly quenched on addition of DNA. Again, the fluorescence band maximum of salt **5e** did not shift, whereas bathochromic shifts of 7 nm were observed in the cases of the amines **5a** and **5b**. Interestingly, the addition of DNA to a saturated solution of dye **5a** resulted in an increase in intensity accompanied with a blue shift of the emission maximum. For further comparison, the behavior of 9-bromoacridizinium bromide (**5f**) under these conditions was investigated. On titration of a solution of salt **5f** with DNA, the changes in the UV-absorption and the emission spectra were similar to those observed for the parent compound **5e**. In addition, in preliminary experiments it was observed that irradiation of supercoiled DNA in the presence of the amino-substituted acridizinium salts **5a** and **5b** led to pronounced strand breaks, as determined by gel electrophoresis. The strand breaks were detected after irradiation in the presence of molecular oxygen; however, when oxygen was excluded, the rate of DNA damage increased significantly.

Photolysis: In an analytical run, the photolysis of the tetrafluoroborate salt of acridizinium **5a** in CD_3CN at $\lambda > 385$ nm was monitored by ^1H NMR spectroscopy. A conversion of $>95\%$ was observed after 2 h. ^1H NMR spectroscopy of the reaction mixture showed that the two head-to-tail photodimers **anti-ht-6a** and **syn-ht-6a** were formed as the major products ($>95\%$) in a 1:1 ratio (Figure 10).^[10] Small

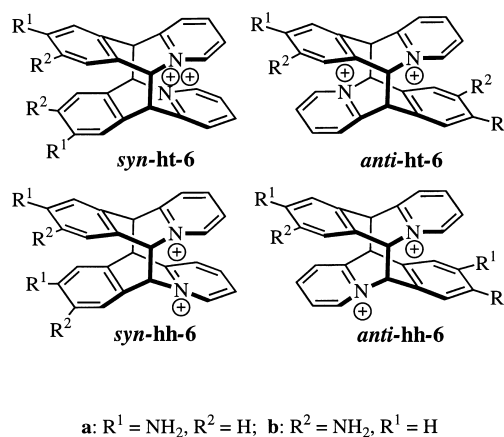


Figure 10. Photodimers **6** of acridizinium salts **5a** and **5b**.

amounts ($<5\%$) of inseparable byproducts were detected in the crude reaction mixture. However, none of the observed signals of these byproducts correspond to a head-to-head dimer, although a very small peak at $\delta = 5.43$ (in CD_3CN , $<1\%$) was noted, which may belong to head-to-head isomers. On standing at room temperature for one day, the small signal disappeared. With bromide as the counter ion, both head-to-tail dimers **anti-ht-6a** and **syn-ht-6a** were also formed as the major products ($>95\%$) on photolysis, as determined by

^1H NMR spectroscopy. The reaction was significantly faster when the counter ion was either tetrafluoroborate or perchlorate. After irradiation for 2.5 h the conversion was 5% in $[\text{D}_6]\text{DMSO}$ and 25% in CD_3OD . Again, a very small peak ($<1\%$) was observed, which may be assigned to a head-to-head dimer. It was also noted that the *anti*-head-to-tail dimer **anti-ht-6a** was preferentially formed (the ratio **anti-ht-6a**:**syn-ht-6a** was 3:1 in $[\text{D}_6]\text{DMSO}$ and 2:1 in CD_3OD). The preference for the *anti*-head-to-tail isomer **anti-ht-6a** is even more pronounced at the beginning of the photoreaction.

The chromatographic isolation of both dimers on silica gel and alumina was difficult due to partial cycloreversion on the stationary phase. One of the dimers could, however, be isolated in small yield as a consequence of its low solubility. Thus, when the acridizinium bromide **5a** was irradiated in deoxygenated methanol for 24 h, one dimer precipitated during the photolysis. The isolated regioisomer was identified as the head-to-tail dimer **anti-ht-6a**. The assignment of the head-to-tail structure of the dimers is based on symmetry considerations. Whereas each bridgehead proton of the head-to-head isomers is expected to give a singlet in the ^1H NMR spectrum, the corresponding protons of the head-to-tail dimers give doublets at lower field. This has been previously shown to be the case for the dimers of the acridizinium salt **5e**.^[16] The investigation of the reaction mixture by ^1H NMR spectroscopy showed two sets of two doublets for the bridgehead protons of the major products ($\delta = 5.85, 5.83, \text{ and } 6.80, 6.83, J = 11 \text{ Hz}$), which are in accord with head-to-tail dimers. Although the regioisomers **anti-ht-6a** and **syn-ht-6a** exhibit essentially identical ^1H NMR spectra, the structures of the *syn* and *anti* isomers could be assigned by comparison with the data for the corresponding head-to-tail dimers of **5e**. By a similar comparison with **5e**, the doublet of the bridgehead proton at C-11 of the *anti* dimer ($\delta = 5.85$) is slightly shifted to lower field relative to the *syn* isomer ($\delta = 5.83$), whereas the reverse situation is found for the protons at C-6 (**anti-ht-6a**: $\delta = 6.80$; **syn-ht-6a**: $\delta = 6.83$). Moreover, in a ROESY-NMR experiment with the dimer mixture, a small NOE effect was observed between the 4-H and 10-H protons and for the 1-H/7-H pair in dimer **anti-ht-6a**. Such NOE effects were not observed for the dimer **syn-ht-6a**.

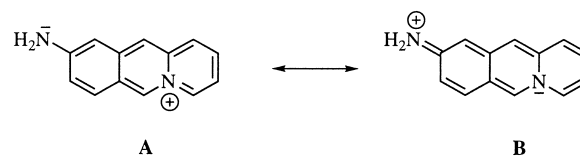
Irradiation of the 8-aminoacridizinium tetrafluoroborate (**5b**) in deoxygenated acetonitrile gave one major product, whose structure was assigned to the head-to-tail dimer **anti-ht-6b**. Smaller amounts of the two head-to-head dimers **anti-hh-6b** and **syn-hh-6b** were also observed. Again, the structural assignment is based on the multiplicity of the bridgehead protons in the ^1H NMR spectrum, in which a doublet with a coupling constant of 11 Hz is consistent with the head-to-tail dimer and singlets in accord with head-to-head structures. On standing at room temperature in acetonitrile solution, the two head-to-head dimers **anti-hh-6b** and **syn-hh-6b** revert to the monomer within 24 h. Since the thermal lability of the dimers **anti-hh-6b** and **syn-hh-6b** may also affect the observed product ratio of the photolysis, the reaction progress was monitored by ^1H NMR spectroscopy. After 30 min irradiation of salt **5b** at $\lambda > 385 \text{ nm}$ in CD_3CN , an **anti-ht-6b**/(**anti-hh-6b** + **syn-hh-6b**) ratio of 0.9:1 was observed with a 3:1 ratio of head-to-head dimers (10% conversion). After one hour, the

ratio changed to 1.1:1 (19% conversion), with a 2:1 ratio of head-to-head dimers. However, extended photolysis for three days resulted in the exclusive formation of the dimer **anti-hh-6b**. To perform this prolonged reaction on a preparative scale, reasonably pure and carefully degassed acetonitrile (UV grade) had to be used to avoid decomposition to unidentified products. The *anti* structure of the head-to-tail dimer **anti-hh-6b** was confirmed by ROESY NMR experiments, which showed a NOE effect between the superposed proton pairs 1-H/7-H and 4-H/10-H. For the head-to-head dimers, it did not prove possible to distinguish between the *syn* and *anti* forms.

Discussion

The introduction of a donor–acceptor system into the acridizinium chromophore resulted in the expected red shift of the absorption relative to the yellow parent compound **5e**.^[14] In addition, the two known amino-substituted acridizinium salts **5g** and **5h** are also reported to be yellow in the solid state.^[17] Although the salts **5g** and **5h** show a red shift in the solution absorption spectra ($\lambda = 418$ and 425 nm) relative to the parent compound **5e**, there is no mention of an absorption tail up to 500 nm or of the appearance of a red color as observed with isomers **5a** and **5b**. The pronounced red shift of the absorption of the substances **5a** and **5b**, relative to the isomers **5g** and **5h**, may result from the higher extended π system between the donor and acceptor functionalities. Such a correlation has already been established for cyanine dyes.^[2] The observation that substitution of the acridizinium salt at the 9-position results in a more pronounced change of absorption properties than substitution with the same functionality at the 6- or 11-positions is quite remarkable, since it has been previously shown that substituents at the 9-position of acridizinium salts usually do not significantly change the absorption properties.^[18]

The absorption properties of chromophore **5a** may be explained on the basis of the two resonance forms **A** and **B** (Scheme 2). Thus, in the ground state, structure **A** may be



Scheme 2. Canonical forms of acridizinium salt **5a**.

more favored, whereas the first excited state is better represented by structure **B**. The energy difference between these canonical forms determines the absorption shift, as has been demonstrated for cyanine dyes.^[1,2] However, such mesomeric forms cannot be drawn for compound **5b**, since there is no conjugation between the two nitrogen atoms. The observation of unexpected absorption properties of dyes with non-conjugated donor–acceptor-substituted π systems compared with their conjugated isomers has already been noted by Heilbronner and Grinter.^[19] Moreover, it has been shown

that acceptor substituents in such systems display a pronounced inductive and only a negligible mesomeric effect.^[20] We conclude that the acridizinium structure in salts **5a** and **5b** acts as an inductively electron-withdrawing group independent of the π conjugation with the corresponding amino functionality. Thus, an intramolecular charge transfer from the amine substituent to the aromatic site on excitation may be responsible for the absorption properties of the two chromophores **5a** and **5b**. This supposition was confirmed by AM1 calculations. Comparison of the net atomic charge distributions in the ground and excited state reveal that a significant shift of electron density occurs from the amine to the acridizinium functionality (mainly into the central ring) on excitation of the chromophore (Table 2).

Table 2. Net atomic charges of acridizinium salts **5a**, **5b**, and **5e** derived from AM1 calculations.

	5a (GS ^[b])	5a (ES ^[c])	5b (GS)	5b (ES)	5e (GS)	5e (ES)
C-1 ^[a]	0.056	0.036	0.079	0.021	0.061	0.051
C-2	0.103	0.128	0.088	0.170	0.098	0.165
C-3	0.089	0.041	0.113	0.004	0.113	0.028
C-4	0.107	0.162	0.093	0.174	0.103	0.196
N-5	-0.010	0.062	0.058	-0.010	0.028	0.025
C-6	0.217	0.040	0.127	0.062	0.191	0.101
C-7	0.108	0.130	-0.113	0.048	0.051	0.124
C-8	0.013	-0.040	0.180	0.164	0.089	0.079
C-9	0.197	0.146	0.032	-0.069	0.110	0.077
C-10	-0.114	0.063	0.086	0.156	0.039	0.134
C-11	0.040	0.047	0.114	0.034	0.094	0.083
C-11a	0.053	0.029	-0.006	0.089	0.028	0.038
C-6a	-0.108	-0.042	0.037	0.005	-0.045	-0.041
C-10a	0.092	-0.017	-0.035	-0.065	0.020	-0.059
NH ₂	0.161	0.215	0.146	0.228	-	-

[a] Numbering according to Figure 1. [b] GS = ground state. [c] ES = excited state, calculated as a biradical.

As has been proposed, the acridizinium salts **5a** and **5b** show efficient fluorescence properties with reasonable quantum yields, presumably due to the rigid molecular framework which prevents radiationless deactivation by conformational changes. The lower fluorescence quantum yield relative to the parent compound **5e** may be explained by quenching due to intermolecular donor–acceptor interactions between the amino group and the acridizinium fluorophore or by radiationless deactivation of the excited state by competing photodimerization. Moreover, it has already been mentioned that acceptor-substituted aniline derivatives exhibit lower fluorescence quantum yields than analogous derivatives without donor–acceptor interplay.^[22b] The amino-substituted acridizinium salts **5a** and **5b** show a significant red shift of the fluorescence relative to the parent compound **5e**, which is a common feature of donor–acceptor-substituted fluorophores.^[21] Although this property may result from an intramolecular charge transfer in the excited state as has been shown by AM1 calculations (Table 2), we exclude a twisted internal charge transfer (TICT),^[22] because the red shift of the emission does not correlate with increasing solvent polarity, a common feature of TICT states. This observation is not surprising because only few cationic dyes exhibit such TICT emission properties.^[22] The observation that the acridizinium

salt **5a** with the “conjugated” donor and acceptor functionalities emits at shorter wavelength than the isomer **5b** is in good agreement with the known red-shifted emission of derivatives substituted at the *ortho* and *meta* positions with donor–acceptor groups compared with their *para*-isomers.^[23] As has been observed for other dyes, a significant red shift of the emission combined with a decrease of intensity results from aggregation of the dye molecules in concentrated solutions.^[24]

In both cases, a weak short-wavelength fluorescence around 440 nm was observed in some solvents. Such an “anti-Stokes shift” is known for some dyes and may be explained by the emission from higher excited states.^[1b] However, this emission is in the spectral range of the fluorescence of the unsubstituted acridizinium salt **5e** and may be the fluorescence of the electronically undisturbed acridizinium fluorophore. Such an emission may result from partial reduction of the donating ability of the amino group by interaction between the solvent and the electron lone pair. In the case of acridizinium salt **5b**, it was shown that in DMF and DMSO solutions the blue-shifted emission is caused by a decomposition product that was detected by the time-dependent appearance of new fluorescence bands along with the decrease of the long-wavelength signals at $\lambda = 560$ nm. However, this emission is likely to have another origin than that observed in protic solvents, because the emission spectra in the latter solvents did not change on standing for extended periods.

The aminoacridizinium salts **5a** and **5b** exhibit a moderate solvatochromism for their absorption and emission properties. A reasonable correlation was not found in either case between the absorption and emission band shifts and the solvent polarity, as expressed by the E_T value.^[25] A difference was observed in the absorption spectra of compounds **5a** and **5b** when recorded in protic and aprotic solvents. For both salts a satisfactory correlation of the absorption band shift with the acceptor number (i.e., electron-accepting properties) of the protic solvents was found, whilst the shifts in aprotic solvents correlate with the donor number, that is electron-donating properties (Figures 11 and 12).^[26] Protic solvents induce a blue shift of the absorption with increasing acceptor number, presumably due to hydrogen bonding to the amine function-

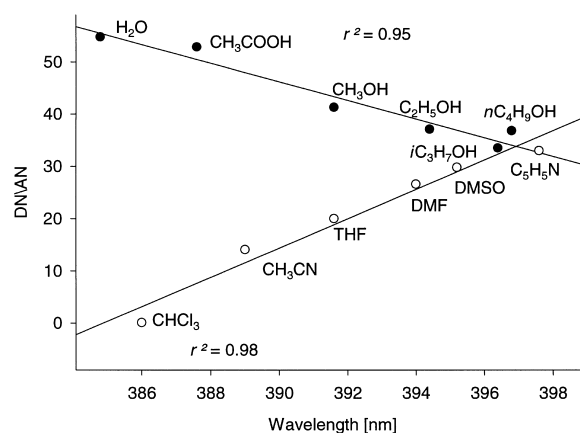


Figure 11. Correlation of the UV-absorption band shifts of acridizinium salt **5a** with the donor (●) and acceptor (○) number of the solvent.

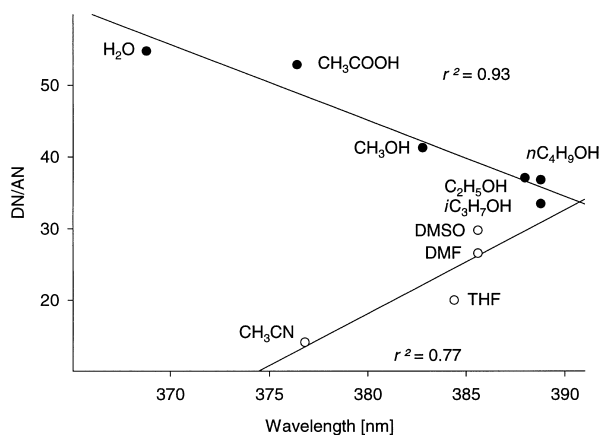


Figure 12. Correlation of the UV-absorption band shifts of acridizinium salt **5b** with the donor number (●) and acceptor (○) of the solvent.

ality. This observation resembles the blue shift anomaly found for aniline and its derivatives.^[26] In contrast, the absorption band shifts to lower wavelength with an increase of the donor number of aprotic solvents. This may be explained by an increasing dipole moment in the excited state. Thus, the excited-state species has greater stabilization in a solvent with pronounced electron-donating abilities and consequently leads to a red shift of the absorption spectrum. In fact, DFT calculations show that the dipole moment of the salt **5a** increases from 0.81 to 8.32 Debye on excitation. It should be noted that the stabilization of the excited state may also result from hydrogen bonding to the amine hydrogen atoms, since it is well-known that the acidity of amines increases significantly on excitation.^[27]

The fluorescence band shifts of acridizinium salts **5a** and **5b** show no correlation with most of the common solvent parameters, namely the E_T value, polarity function $f(D)$, or the dipole moment μ .^[25] Similar results have been noted for other dyes such as proflavin and acridine orange,^[28] although in these examples a reasonable correlation of the Stokes shifts with refractive index was observed. In the case of the acridizinium salt **5a**, the emission properties in alcohol solutions and in water are roughly the same. In aprotic solvents a moderate correlation with the donor number of the solvent was observed (Figure 13). Although there is a good

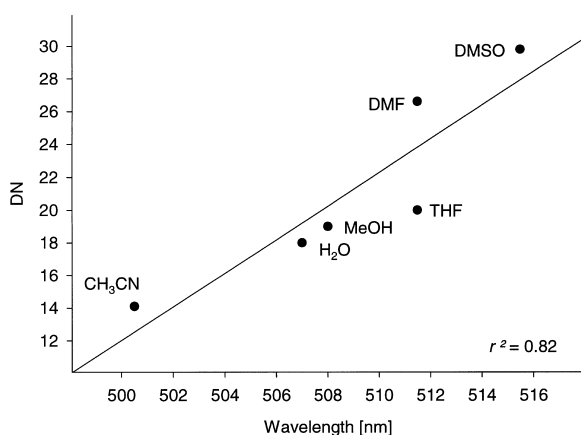


Figure 13. Correlation of the fluorescence band shifts of acridizinium salt **5a** with the donor number of the solvent.

correlation in methanol and water, significant deviations are found in other alcohols. This observation may be explained by the fact that the determination of the donor number for alcohols is rather erroneous.^[29] With increasing donor number of the solvent, the emission is red shifted corresponding to a greater stabilization of the excited state, presumably due to the same mechanism responsible for solvatochromism of the absorption spectrum. The same correlation was observed for the 8-amino-substituted acridizinium salt **5b** (Figure 14), although the spectra in alcoholic solvents show a larger difference compared with those of the 9-isomer **5a**.

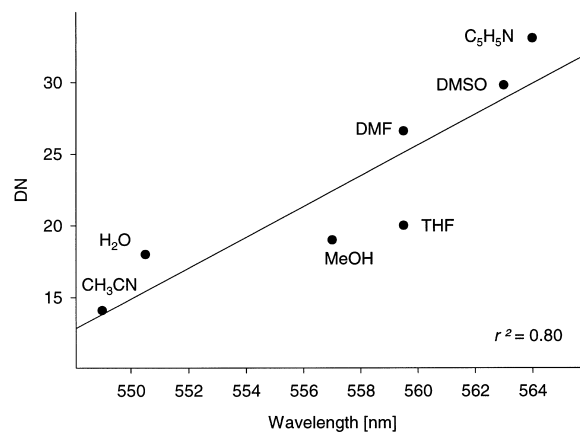


Figure 14. Correlation of the fluorescence band shifts of acridizinium salt **5b** with the donor number of the solvent.

Since the acridizinium salts **5a** and **5b** exhibit reasonably efficient fluorescence properties that are sensitive towards their environment, we investigated their potential as fluorescence probes in biological systems. Thus, titration of the fluorophores **5a** and **5b** with DNA not only quenched the absorption and fluorescence, but caused also a significant shift of the emission maximum. Similar results have previously been obtained by UV-monitored titration of DNA with coralyne, a benzo-annulated acridizinium derivative,^[30] and with other quinolizinium derivatives.^[31] From these preliminary results we propose that the amino-substituted acridizinium salts **5a** and **5b** interact with DNA and that the associated environmental changes shift the absorption and the emission bands. This postulate is supported by the observation that the addition of DNA to more concentrated solutions of amine **5a** resulted in an increase of the emission intensity and in a blue shift. Since the long-wavelength emission and the low fluorescence intensity of the concentrated solution is caused by aggregation of the dye molecules,^[24] it may be concluded that these aggregates are dissociated on DNA addition due to strong interactions of the dye with the DNA molecules. At this time it is still unclear whether the strong interaction of the salts **5a** and **5b** with DNA results from association with the ionic phosphate backbone, binding to the major or minor groove, or intercalation, and further experiments will be required to resolve this question. However, since no shift of the emission band was observed on DNA addition to the parent compound **5e** and to 9-substituted acridizinium salt **5f**, it is apparent that the introduction of the amine functionality

into the acridizinium chromophore enhances the sensitivity of the photophysical properties towards the environment. This property may be useful for the application of the dyes **5a** and **5b** as photobiological fluorescence probes.

The regioselective photodimerization of acridizinium salt **5a** is surprising, because in all cases in which the photolysate of acridizinium salts have been carefully investigated, such a selectivity on photolysis in solution has not been observed.^[16, 32] Nevertheless, there are reports of regioselective head-to-tail dimerizations of other aza-heterocyclic aromatic compounds^[33] and of a 2,6-donor–acceptor-substituted anthracene.^[34] The selectivity of the dimerization may be due to the thermal lability of the head-to-head isomers, since ¹H NMR spectroscopy indicated that very small amounts of head-to-head isomers are formed on photolysis, which then smoothly cyclorevert at room temperature. Since these dimers may be detected by NMR spectroscopy, they should be sufficiently long lived to permit their observation. However, when the reaction was monitored by ¹H NMR spectroscopy there did not appear to be any enhanced formation of these head-to-head dimers. To explore further the thermal stability of head-to-tail photodimers of 9-substituted acridizinium salts in general, we examined the photolysis of 9-bromoacridizinium bromide^[32] (**5f**), in which the two head-to-head dimers are formed in about 25% yield. ¹H NMR spectroscopy revealed no significant decomposition of the head-to-head dimers after standing at room temperature for two days. From these results we conclude that the observed regioselectivity of the photodimerization of 9-aminoacridizinium salt (**5a**) is unlikely to be caused by the thermal lability of the head-to-head dimers.

The regioselectivity of the photocycloaddition reaction should result from the favored alignment of the excited- and ground-state acridizinium molecules during excimer formation. According to frontier molecular orbital (FMO) control, the HOMO–HOMO and LUMO–LUMO interactions between the ground- and excited-state molecules should lead to head-to-head arranged excimers, which in turn lead to the corresponding photodimers.^[35] DFT calculations of the acridizinium salt **5a** reveal that, indeed, HOMO–HOMO interactions favor head-to-head dimers owing to significant differences in the orbital coefficients at the 6- and 11-position (Figure 15); however, the coefficients of the LUMO at these positions are very similar. Thus, a LUMO–LUMO interaction does not necessarily lead to a head-to-head dimer. Since the acridizinium salt **5a** is a positively charged compound, the net atomic-charge distributions within the molecule in the ground and excited states were also calculated to assess whether the regioselective photodimerization may be due to attractive or repulsive charge interactions. AM1 calculations

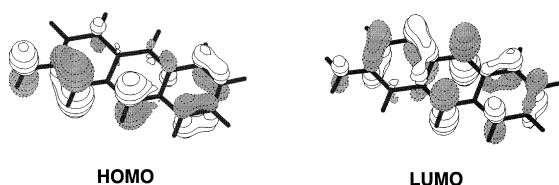


Figure 15. HOMO and LUMO orbital coefficients of acridizinium salt **5a** from DFT calculations.

indicate that in the excited state the net atomic charges at the relevant positions, that is C-6 and C-11, are nearly equal (Table 2). Thus, based on attractive or repulsive charge interactions, there should be no preference for an approach to the 6- or 11-positions. From these computational data it may be deduced that the regiochemistry of the present photodimerization is not influenced by electrostatic and orbital interactions between excited- and ground-state molecules, although the geometry of the initially formed excimers will be controlled by such interactions.

According to FMO theory, photodimerizations should yield head-to-head isomers.^[35] Nevertheless, in some cases head-to-tail products are also formed. From detailed theoretical studies on the [2+2] photodimerization of substituted alkenes, a conical intersection has been detected with an energy minimum for a head-to-tail arrangement, which determines the regioselectivity of the reaction.^[36] Since the same theoretical considerations have been used to explain the electronic influence of substituents on the head-to-tail photocyclization of anthracene derivatives,^[36] and a conical intersection has also been found recently for the [4+4] photocyclization of 1,3-butadiene,^[37] it is tempting to assume that a conical intersection with a head-to-tail geometry of the ground and excited states of salt **5a** exist on the hypersurfaces. This conical intersection thus determines the regioselectivity of the photodimerization independently from the regioselectivity of the excimer formation.

Photolysis of acridizinium salt **5b** yielded the head-to-head photodimers *anti*-**hh-6b** and *syn*-**hh-6b**, along with the head-to-tail dimer *anti*-**ht-6b**. The dimers *anti*-**hh-6b** and *syn*-**hh-6b** exhibit a remarkable thermal lability, and the selective formation of the head-to-tail dimer *anti*-**ht-6b** on prolonged irradiation is the result of thermodynamic control. The thermal lability of the head-to-head dimers may be explained in terms of two stabilized capto-dative radical centers in diradical **7** (Figure 16), which result from the cleavage of the C11–C11' bond in dimers *anti*-**hh-6b** and *syn*-**hh-6b**. Such capto-dative radicals are known to be quite stable and easily formed.^[38] The diradical **7** may recombine to the dimer or revert to the monomers on further cleavage of the C6–C6' bond. Attempts to trap the radicals with thiols or methyl

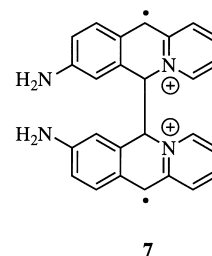


Figure 16. Structure of biradical **7**.

acrylate failed. Significantly, the formation of the *syn*-head-to-tail dimer was not observed under the reaction conditions, and it is not clear whether this dimer is thermally or photochemically labile or even if it is indeed formed during the photolysis. To assess whether the lability of the head-to-head dimers and the absence of a *syn*-head-to-tail dimer are general features of the so far unexplored photochemistry of 8-substituted acridizinium photolysis, the known 8-hydroxyacridizinium salt^[11] was irradiated in DMSO and methanol. On monitoring the reaction progress by ¹H NMR spectroscopy, all four regioisomers were observed. Moreover, the head-to-head dimers did not revert to the monomer on standing at room

temperature. Thus, the lability of the head-to-head dimers of the 8-aminoacridizinium salt **5b** must arise from the amino substitution. Since isomer **5b** is not regioselectively photodimerized like the acridizinium salt **5a**, it may be concluded that the selectivity of the photodimerization of salt **5a** results from the conjugated donor–acceptor interaction.

It is worth mentioning that the dimers *anti*-**ht-6a,b** are colored species due to a broad absorption tail into the visible region.^[39] This so far unprecedented color of acridizinium dimers may be due to an intramolecular charge transfer between the aniline moiety and the superposed pyridinium ring.

In conclusion, we have shown that the novel acridizinium based dyes **5a** and **5b** exhibit a pronounced color and efficient fluorescent properties with reasonable quantum yields. The sensitivity of the photophysical properties towards the medium, combined with the efficacy of the fluorescence, may be of practical use for fluorescence sensing. Moreover, it has been shown that these dyes may also be of photo-biological interest owing to their interaction with DNA. The exceptional regioselectivity in the [4+4] photodimerization of acridizinium salt **5a** provides good possibilities for the enhancement of the regioselectivity of photocycloaddition reactions by incorporating the chromophore within a conjugated donor–acceptor system. Since the donor–acceptor interaction is efficiently blocked in the photodimers *anti*-**ht-6a** and *syn*-**ht-6a**, such photochromic systems may also serve as new switchable materials for NLO activity or photo-refractive effects.^[40]

Experimental Section

¹H NMR and ¹³C NMR spectroscopy: Bruker AC200 (¹H NMR: 200 MHz; ¹³C NMR: 50.3 MHz); Bruker DMX600 (¹H NMR: 600 MHz, ROESY experiments). C_q, CH, CH₂, and CH₃ were determined by using the DEPT pulse sequence. ¹H NMR chemical shifts refer to δ_{TMS}=0.0 or solvent signals ([D₆]DMSO: δ = 2.59; CD₃CN: δ = 1.94). ¹³C NMR chemical shifts refer to solvent signals ([D₆]DMSO: δ = 39.5; CD₃CN: δ = 1.3, 118.1). UV: Hitachi U-3200 spectrophotometer. Fluorescence: Perkin Elmer LS50 spectrometer; solid-state fluorescence spectra were recorded with a Front Surface Accessory, Perkin Elmer. Fluorescence spectra were treated with the “smooth” command (factor 5) as implemented in the Perkin Elmer Fluorescence Data Manager. MS: Varian MAT 731. We would like to thank Dr. Remberg, Universität Göttingen, for recording of the FAB mass spectra. Melting points are uncorrected. Elemental analyses were performed by C.-P. Kneis, Mikroanalytisches Labor der Universität Würzburg, Institut für Anorganische Chemie. Photoreactions were performed with a high-pressure mercury lamp (150 W, Heraeus TQ150) at room temperature; the samples were placed about 5 cm in front of the cooling mantle of the light source. A glass filter (Schott GG385; λ > 385 nm) was placed between the sample and the light source. Absorption and emission spectra were recorded in deoxygenated spectral grade solvents (Fluka). Distilled water was further deionized by employing Millipore MilliQ equipment. If not stated otherwise, the solution concentrations were 10⁻⁴ M for absorption spectroscopy and 10⁻⁵ M for fluorescence spectroscopy. Emission spectra were recorded with an excitation wavelength close to the absorption maximum (λ = 380 nm). The relative fluorescence quantum yields were determined by the standard method^[41] with quinine sulfate in 1 N H₂SO₄ as reference (φ_{Fl} = 0.546^[42]). Solution photolyses were carried out in deoxygenated spectral grade solvents, which were purged with argon gas for at least 30 min prior to use. *Calif thymus* DNA was purchased from Merck and dissolved in deionized water (1 mg mL⁻¹). The actual concentration was determined by UV spectroscopy relative to a calibrated *calif thymus* DNA

solution (50 μg mL⁻¹) whose absorbance equals 1 at λ = 260 nm. Semi-empirical calculations were performed on a Silicon Graphics Iris Indigo R4000 workstation. AM1 parameters^[43] were taken as provided by the VAMP program, version 6.1.^[44] For the determination of the net atomic charges of hydrogen-substituted atoms X–H (X = C or N), the overall charge of the X–H moiety was taken.

2-(1,3-Dioxolan-2-yl)-N-(4'-phthalimidylbenzyl)pyridinium bromide (4a): A solution of *N*-(4-bromomethylphenyl)phthalimide^[45] **2a** (1.254 g, 3.97 mmol) and 2-(1,3-dioxolan-2-yl)pyridine^[46] **3** (596 mg, 3.97 mmol) in DMSO (10 mL) was stirred under an on atmosphere at room temperature for 7 d. The pyridinium derivative **4a** was precipitated by slow addition of ethyl acetate with rapid stirring. The product was washed with ethyl acetate and recrystallized from methanol to give salt **4a** (993 mg, 2.12 mmol, 53 %) as white crystals. M.p. 182–183 °C (decomp); ¹H NMR (CD₃OD): δ = 4.22 (s, 4H, CH₂), 6.13 (s, 2H, CH₂), 6.47 (s, 1H, CH), 7.51–7.62 (m, 4H, ar-H), 7.86–7.98 (m, 4H, ar-H), 8.15 (dd, ³J = 7 Hz, ³J = 6 Hz, 1H, ar-H), 8.43 (d, ³J = 7 Hz, 1H, ar-H), 8.71 (dd, ³J = 7 Hz, ³J = 7 Hz, 1H, ar-H), 8.99 (d, ³J = 6 Hz, 1H, ar-H); ¹³C NMR (CD₃OD): δ = 61.6 (CH₂), 67.4 (CH₂), 99.0 (CH), 124.7 (CH), 127.5 (CH), 128.9 (CH), 129.7 (CH), 130.4 (CH), 133.0 (C_q), 133.9 (C_q), 134.6 (C_q), 135.9 (CH), 148.3 (CH), 148.5 (CH), 168.5 (C=O), one ar-C_q not detected; MS (FAB (+), glycerol): *m/z* (%): 387 (83) [*M*]⁺; elemental analysis calcd (%) for C₂₃H₁₉BrN₂O₄·H₂O (485.3): C 56.92, H 4.36, N 5.77; found C 57.02, H 4.44, N 5.51.

9-Phthalimidylacridizinium tetrafluoroborate (5c) and 9-aminoacridizinium tetrafluoroborate (5a): The pyridinium salt **4a** (742 mg, 1.59 mmol) was added in small portions to polyphosphoric acid (15 g, 84 %) at 80 °C. The viscous solution was stirred slowly at 90 °C for 14 h. Water (20 mL) was carefully added, the solution stirred at 80 °C for 30 min, then cooled to room temperature, and washed with chloroform (50 mL). Tetrafluoroboric acid (5 mL, 50 %) was added slowly to the aqueous phase. The resulting yellow-orange precipitate was collected by filtration and washed with water (10 mL). The remaining solid was extracted with methanol to afford phthalimidylacridizinium tetrafluoroborate (**5c**) (35 mg, 0.08 mmol, 5 %) as an insoluble peach-colored solid. From the filtrate 9-aminoacridizinium tetrafluoroborate (**5a**) crystallized –4 °C as red small needles (203 mg, 0.72 mmol, 45 %).

Compound 5c: M.p. 282–286 °C (decomp); UV/Vis (MeOH): λ (log ε) = 212 (4.52), 249 (4.47), 260 (4.45), 298 (4.46), 386 (4.09), 411 nm (3.93); ¹H NMR (200 MHz, [D₆]DMSO): δ = 8.06–8.26 (m, 7H, ar-H), 8.60–8.75 (m, 3H, ar-H), 9.42 (d, ³J = 7 Hz, 1H, ar-H), 9.43 (s, 1H, ar-H), 10.58 (s, 1H, ar-H); ¹³C NMR ([D₆]DMSO): δ = 122.4 (CH), 123.3 (CH), 123.8 (C_q), 124.3 (CH), 124.8 (CH), 126.8 (CH), 129.1 (CH), 129.7 (CH), 131.4 (CH), 134.4 (CH), 135.1 (CH), 136.8 (C_q), 137.7 (C_q), 140.2 (CH), 151.9 (C_q), 166.4 (CH); elemental analysis calcd (%) for C₂₁H₁₃B₁F₄N₂O₂·0.5H₂O (421.2): C 59.89, H 3.35, N 6.65; found C 60.24, H 3.27, N 6.75.

Compound 5a: M.p. 221–225 °C (decomp); UV/Vis (MeOH): λ (log ε) = 226 (4.19), 257 (4.47), 294 (4.45), 391 nm (4.28); ¹H NMR (200 MHz, [D₆]DMSO): δ = 7.01 (d, ⁴J = 2 Hz, 1H, 10-H), 7.46–7.54 (m, 2H, 3-H, 8-H), 7.75 (dd, ³J = 9 Hz, ³J = 7 Hz, 1H, 2-H), 8.12 (d, ³J = 9 Hz, 1H, 1-H), 8.21 (d, ³J = 9 Hz, 1H, 7-H), 8.40 (s, 1H, 11-H), 8.85 (d, ³J = 7 Hz, 1H, 4-H), 9.83 (s, 1H, 6-H); ¹³C NMR ([D₆]DMSO): δ = 99.9 (CH), 116.6 (CH), 118.2 (CH), 120.2 (C_q), 124.9 (CH), 125.2 (CH), 129.4 (CH), 130.5 (CH), 133.4 (CH), 137.3 (C_q), 138.2 (C_q), 138.5 (CH), 154.9 (C_q); MS (FAB (+), glycerol): *m/z* (%): 195 (8) [*M*]⁺; elemental analysis calcd (%) for C₁₃H₁₁BF₄N₂ (282.05): C 55.36, H 3.93, N 9.93; found C 55.63, H 3.87, N 9.65.

2-(1,3-Dioxolan-2-yl)-N-(3'-phthalimidylbenzyl)pyridinium bromide (4b): A solution of *N*-(3-bromomethylphenyl)phthalimide^[47] (**2b**) (2.90 g, 9.2 mmol) and 2-(1,3-dioxolan-2-yl)pyridine (**3**) (2.00 g, 13.3 mmol) in DMSO (10 mL) was stirred under an argon atmosphere at room temperature for 6 d. The pyridinium derivative **4b** was precipitated by slow addition of ethyl acetate with vigorous stirring. The precipitate was washed twice with ethyl acetate and recrystallized from methanol/ethyl acetate to yield salt **4b** (2.50 g, 5.3 mmol, 58 %) as white needles. M.p. 165–167 °C (decomp); ¹H NMR (200 MHz, [D₆]DMSO): δ = 4.20 (s, 4H, CH₂), 6.19 (s, 2H, CH₂), 6.60 (s, 1H, CH), 7.46–7.74 (m, 4H, ar-H), 7.98–8.08 (m, 4H, ar-H), 8.31–8.44 (m, 2H, ar-H), 8.84 (dd, ³J = 8 Hz, ³J = 8 Hz, 1H, ar-H), 9.25 (d, ³J = 6 Hz, 1H, ar-H); ¹³C NMR ([D₆]DMSO): δ = 59.6 (CH₂), 65.6 (CH₂), 97.1 (CH), 123.5 (CH), 126.2 (CH), 126.4 (CH), 127.5 (CH), 127.7 (CH), 128.7 (CH), 129.5 (CH), 131.4 (C_q), 132.5 (C_q), 134.8 (CH), 134.8

(C_q), 147.4 (CH), 147.6 (CH), 152.2 (C_q), 166.8 (C_q); MS (FAB (+), 3-nitrobenzyl alcohol): *m/z* (%): 387 (100) [M]⁺; elemental analysis calcd (%) for C₂₃H₁₉BrN₂O₄ (467.32): C 58.73, H 4.10, N 5.99; found C 58.73, H 3.62, N 6.10.

8-Phthalimidylacridizinium tetrafluoroborate (5d) and 8-aminoacridizinium tetrafluoroborate (5b): The pyridinium salt **4b** (870 mg, 1.86 mmol) was added in small portions to polyphosphoric acid (20 g, 84%) and the mixture stirred for 20 h at 90 °C. Water (20 mL) was added, the solution stirred at 90 °C for 30 min and then cooled to room temperature. After the filtration of small amounts of a white solid, the filtrate was treated with HBF₄ (ca. 5 mL, 50%) to precipitate the phthalimidylacridizinium salt **5d**, which was removed by filtration and crystallized from methanol to give phthalimide **5d** (27 mg, 0.06 mmol, 3%) as a yellow powder. The filtrate was neutralized with Na₂HPO₄ to afford a red solid. The solid was collected by filtration, washed with water (5 mL), and crystallized twice from methanol to give salt **5b** (283 mg, 0.86 mmol, 37%) as small red crystals.

Compound 5d: M.p. 251–259 °C (decomp); UV/Vis (MeOH): λ (log ε) = 216 (4.59), 262 (4.43), 292 (4.20), 345 (3.83), 364 (3.97), 394 nm (3.61); ¹H NMR (200 MHz, [D₆]DMSO): δ = 8.05–8.35 (m, 7H, ar-H), 8.62–8.74 (m, 3H, ar-H), 9.39 (d, ³J = 7 Hz, 1H, ar-H), 9.40 (s, 1H, ar-H), 10.65 (s, 1H, ar-H); ¹³C NMR ([D₆]DMSO): δ = 122.7 (CH), 123.7 (CH), 124.8 (CH), 124.8 (CH), 125.7 (C_q), 127.0 (CH), 128.2 (CH), 131.4 (C_q), 131.6 (CH), 133.5 (C_q), 133.6 (C_q), 134.0 (CH), 134.4 (CH), 135.1 (CH), 137.8 (C_q), 140.5 (CH), 166.6 (C=O); MS (FAB (+), 3-nitrobenzyl alcohol): *m/z* (%): 325 (100) [M]⁺.

Compound 5b: M.p. 222–225 °C (decomp); UV/Vis (MeOH): λ (log ε) = 219 (4.27), 247 (4.34), 282 (4.36), 312 (4.52), 321 (4.51), 382 nm (4.13); ¹H NMR (200 MHz, [D₆]DMSO): δ = 6.82 (brs, 2H, NH₂), 7.12 (d, ⁴J = 2 Hz, 1H, 7-H), 7.68 (dd, ³J = 9 Hz, ⁴J = 2 Hz, 1H, 9-H), 7.84–7.89 (m, 2H, 1-H, 3-H), 8.23 (d, ³J = 7 Hz, 1H, 10-H), 8.40–8.46 (m, 1H, 2-H), 8.96 (s, 1H, 11-H), 9.06–9.10 (m, 1H, 4-H), 9.91 (s, 1H, 6-H); ¹³C NMR ([D₆]DMSO): δ = 99.2 (CH), 122.1 (CH), 124.2 (CH), 126.9 (CH), 127.7 (CH), 128.5 (CH), 129.1 (C_q), 129.3 (CH), 130.0 (C_q), 132.6 (CH), 133.6 (CH), 134.0 (C_q), 150.9 (C_q); MS (FAB (+), 4-nitrobenzyl alcohol): *m/z* (%): 195 (47) [M]⁺; elemental analysis calcd (%) for C₁₃H₁₁BF₄N₂ (282.05): C 55.36, H 3.93, N 9.93; found C 55.53, H 3.96, N 10.12.

Photodimerization of 9-aminoacridizinium bromide (5a): A solution of acridizinium bromide **5a** (71 mg, 0.26 mmol) in deoxygenated methanol (10 mL) was irradiated at λ > 385 nm for 24 h. A solid precipitated during the photolysis was removed by filtration and washed twice with methanol (2 mL) to give dimer **anti-ht-6a** (22 mg) as a yellow powder. A further quantity of the dimer **anti-ht-6a** (13 mg) was isolated by crystallization from methanol (total yield: 5 mg, 0.06 mmol, 48%).

Compound anti-ht-6a: M.p. 265–272 °C (decomp); UV/Vis (MeOH): λ (log ε) = 208 (4.56), 254 (4.59), 313 nm (3.64); ¹H NMR (200 MHz, [D₆]DMSO): δ = 5.63 (brs, 2H, NH₂), 5.85 (d, ³J = 11 Hz, 2H, 11-H, 11'-H), 6.39 (dd, ³J = 8 Hz, ²J = 2 Hz, 2H, 8-H, 8'-H), 6.60 (d, ²J = 2 Hz, 10-H, 10'-H), 6.80 (d, ³J = 11 Hz, 2H, 6-H, 6'-H), 7.04 (d, ³J = 8 Hz, 2H, 7-H, 7'-H), 8.00 (dd, ³J = 8 Hz, ³J = 6 Hz, 2H, 3-H, 3'-H), 8.14 (d, ³J = 7 Hz, 2H, 1-H, 1'-H), 8.52 (dd, ³J = 8 Hz, ³J = 7 Hz, 2H, 2-H, 2'-H), 9.15 (d, ³J = 6 Hz, 2H, 4-H, 4'-H); ¹³C NMR ([D₆]DMSO): δ = 50.6 (C-11), 71.4 (C-6), 112.6 (CH), 112.7 (CH), 120.0 (C_q), 126.0 (CH), 128.1 (CH), 128.6 (CH), 133.7 (C_q), 145.3 (CH), 146.5 (CH), 149.9 (C_q), 154.3 (C_q).

Compound syn-ht-6a (pair of enantiomers; data determined from the mixture with **anti-ht-6a**): ¹H NMR (200 MHz, [D₆]DMSO): δ = 5.63 (brs, 2H, NH₂), 5.83 (d, ³J = 10 Hz, 2H), 6.44 (dd, ³J = 8 Hz, ²J = 2 Hz, 2H), 6.60 (d, ³J = 2 Hz, 2H), 6.83 (d, ³J = 11 Hz, 2H), 7.10 (d, ³J = 8 Hz, 2H), 8.00 (dd, ³J = 8 Hz, ³J = 6 Hz, 2H), 8.17 (d, ³J = 7 Hz, 2H), 8.50 (dd, ³J = 8 Hz, ³J = 7 Hz, 2H), 9.12 (d, ³J = 6 Hz, 2H); ¹³C NMR ([D₆]DMSO): δ = 50.5 (C-11), 72.6 (C-6), 112.4, 113.1, 120.5, 126.7, 128.2, 128.9, 134.7, 145.6, 147.0, 149.1, 152.9.

Photodimerization of 8-aminoacridizinium tetrafluoroborate (5b): A solution of acridizinium salt **5b** (25 mg, 0.09 mmol) in rigorously deoxygenated acetonitrile (10 mL) was irradiated at λ > 385 nm for 3 d. A ¹H NMR spectroscopic investigation of the crude reaction mixture showed that dimer **anti-ht-6b** was formed as the major product along with traces of unidentified byproducts (71% conversion). The solvent was removed in vacuo and the resulting solid washed twice with methanol (5 mL) to give dimer **anti-ht-6b** (10 mg, 0.02 mmol, 58% yield based on 71% conversion) as a red amorphous solid. M.p. 242–246 °C (decomp); UV/Vis (CH₃CN): λ

(log ε) = 192 (4.48), 206 (sh, 4.28), 250 (4.13), 267 (sh, 4.01), 312 (3.59), 375 nm (3.14); ¹H NMR (200 MHz, CD₃CN): δ = 4.50 (brs, 4H, NH₂), 5.64 (d, ³J = 10 Hz, 2H, 6-H, 6'-H), 6.39 (dd, ³J = 8 Hz, ²J = 2 Hz, 2H, 9-H, 9'-H), 6.42 (d, ³J = 10 Hz, 2H, 11-H, 11'-H), 6.66 (d, ³J = 10 Hz, 2H, 7-H, 7'-H), 7.03 (d, ³J = 8 Hz, 2H, 10-H, 10'-H), 7.69 (dd, ³J = 8 Hz, ³J = 6 Hz, 2H, 3-H, 3'-H), 7.86 (d, ³J = 8 Hz, 2H, 1-H, 1'-H), 8.27 (dd, ³J = 8 Hz, ³J = 8 Hz, 2H, 2-H, 2'-H), 8.64 (d, ³J = 6 Hz, 2H, 4-H, 4'-H); ¹³C-NMR (CD₃CN): δ = 51.2 (C-11), 74.2 (C-6), 113.4 (CH), 115.6 (CH), 119.1 (C_q), 127.3 (CH), 129.9 (CH), 130.9 (CH), 136.7 (C_q), 146.3 (CH), 147.6 (CH), 150.1 (C_q), 155.7 (C_q).

Acknowledgement

This work was generously financed by the *Bundesministerium für Bildung und Forschung*, the *Deutsche Forschungsgemeinschaft*, and the *Fonds der Chemischen Industrie*. Constant support and encouragement by Prof. Waldemar Adam is gratefully appreciated. We thank Dr. M. Grüne and E. Ruckdeschel for conducting the ROESY-NMR experiments and A. Häfner and Prof. F. W. Schneider for recording the fluorescence lifetimes.

- [1] a) S. Dähne, *Chimia* **1991**, *45*, 288–296; b) N. Tyutyulkov, J. Fabian, A. Mehlhorn, F. Dietz, A. Tadjer, *Polymethine Dyes, Structure and Properties*, St. Kliment Ohridski University Press, Sofia, **1991**; c) D. M. Sturmer, in *Synthesis and Properties of Cyanine Dyes and Related Dyes, Vol. 30* (Eds.: A. Weissberger, E. C. Taylor), Wiley, New York, **1977**; d) H. Zollinger, *Color Chemistry*, VCH, Weinheim, **1988**.
- [2] J. Fabian, H. Hartmann, *Light Absorption of Organic Colorants*, Springer, Berlin, **1980**, pp. 162–197.
- [3] a) J. Rochlitz, *Chimia* **1980**, *34*, 131–144.
- [4] a) M. Maeda, *Laser Dyes. Properties of Organic Compounds for Dye Lasers*, Academic Press, New York, **1984**; b) P. Czerney, G. Graness, E. Birckner, F. Vollmer, W. Rettig, *J. Photochem. Photobiol. A: Chemistry* **1995**, *89*, 31–36.
- [5] a) D. J. Owen, D. Vanderveer, G. B. Schuster, *J. Am. Chem. Soc.* **1998**, *120*, 1705–1717; b) K. B. Simonson, T. Geisler, J. Arentoft, P. Sommer-Larsen, D. R. Greve, C. Jakobson, J. Becher, M. Malagoli, J. L. Bredas, *Eur. J. Org. Chem.* **1998**, 2747–2757; c) *Nonlinear Optics of Organic Molecules and Polymers* (Eds.: H. S. Nalva, S. Miyata), CRC Press, Boca Raton, **1995**.
- [6] a) J. L. Seifert, R. E. Connor, S. A. Kushon, M. Wang, B. A. Armitage, *J. Am. Chem. Soc.* **1999**, *121*, 2987–2995; b) E. Bruns, C. J. Murphy, M. A. Berg, *J. Am. Chem. Soc.* **1998**, *120*, 2449–2456; c) B. Armitage, *Chem. Rev.* **1998**, *98*, 1171–1200; d) I. E. Kochevar, D. D. Dunn, in *Bioorganic Photochemistry* (Ed.: H. Morrison), Wiley, New York, **1990**, pp. 273–315.
- [7] a) A. P. de Silva, H. Q. N. Gunaratne, T. Gunnlaugsson, A. J. M. Huxley, C. P. McCoy, J. T. Rademacher, T. E. Rice, *Chem. Rev.* **1997**, *97*, 1515–1566; b) B. Valeur, in *Topics in Fluorescence Spectroscopy, Vol. 4* (Ed.: J. R. Lakowicz), Plenum, New York, **1994**, pp. 21–50; c) A. W. Czarnik, in *Topics in Fluorescence Spectroscopy, Vol. 4* (Ed.: J. R. Lakowicz), Plenum, New York, **1994**, pp. 51–70.
- [8] J.-M. Lehn, *Supramolecular Chemistry*, VCH, Weinheim, **1995**.
- [9] For other strategies to make the cyanine framework rigid, see for example: a) M. Szczepan, W. Rettig, Y. L. Bricks, Y. L. Slominski, A. I. Tolmachev, *J. Photochem. Photobiol. A* **1999**, *124*, 75–84; b) H. J. Friedrich, W. Guckel, G. Scheibe, *Chem. Ber.* **1962**, *95*, 1378–1387.
- [10] Parts of this work have appeared as a preliminary communication: H. Ihmels, *Tetrahedron Lett.* **1998**, *39*, 8641–8642.
- [11] a) C. K. Bradsher, in *Comprehensive Heterocyclic Chemistry, Vol. 2* (Eds.: A. J. Boulter, A. McKillop), Pergamon, Oxford **1985**, pp. 525–579. b) C. K. Bradsher, J. C. Parham, *J. Heterocyclic Chem.* **1964**, *1*, 30–33.
- [12] S. Kukulja, S. R. Lammert, *J. Am. Chem. Soc.* **1975**, *97*, 5582–5583.
- [13] Concentrated aqueous solutions of salt **5b** show a remarkably low surface tension as indicated by its tendency to stick to glass surfaces.
- [14] S.-U.-D. Saraf, *Heterocycles* **1981**, *16*, 987–1007.
- [15] K. Faulhaber, A. Häfner, H. Ihmels, F. W. Schneider, unpublished results.

- [16] C. Lehnberger, D. Scheller, T. Wolff, *Heterocycles* **1997**, *10*, 2033–2036.
- [17] a) C. K. Bradsher, L. S. Davies, *J. Org. Chem.* **1973**, *38*, 4167–4170; b) C. K. Bradsher, J. P. Sherer, *J. Org. Chem.* **1967**, *32*, 733–737; c) For another amino-substituted acridizinium derivative for which no UV data are reported, see: J. W. H. Wattleby, K. J. Doebel, H. F. Vernay, A. L. Lopano, *J. Org. Chem.* **1973**, *38*, 4170–4172.
- [18] D. L. Kerbow, *Diss. Abstr. B* **1966**, *27*, 382.
- [19] R. Grinter, E. Heilbronner, *Helv. Chim. Acta* **1962**, *45*, 2496–2516.
- [20] T. M. Krygowski, *J. Chem. Soc. Perkin Trans 2* **1989**, 695–698.
- [21] B. M. Krasvitskii, B. M. Bolotin, *Organic Luminescent Materials*, VCH, Weinheim, **1988**.
- [22] a) W. Rettig, *Top. Curr. Chem.* **1994**, *169*, 253–299; b) W. Rettig, *Angew. Chem.*, **1986**, *98*, 969–986; *Angew. Chem. Int. Ed. Engl.*, **1986**, *25*, 971–988.
- [23] T. Förster, *Fluoreszenz Organischer Verbindungen*, Vandenhoeck and Ruprecht, Göttingen, **1982**.
- [24] M. S. Melvin, D. C. Ferguson, N. Lindquist, R. Manderville, *J. Org. Chem.* **1999**, *64*, 6861–6869.
- [25] a) C. Reichardt, *Chem. Rev.* **1994**, *94*, 2319–2358; b) C. Reichardt, *Solvents and Solvent Effects in Organic Chemistry*, 2nd ed., VCH, Weinheim, **1988**.
- [26] P. Suppan, N. Ghoneim, *Solvatochromism*, The Royal Society of Chemistry, London, **1997**.
- [27] J. F. Ireland, P. A. H. Wyatt, *Adv. Phys. Org. Chem.* **1976**, *12*, 131–221.
- [28] a) E. B. Brauns, C. J. Murphy, M. A. Berg, *J. Am. Chem. Soc.* **1998**, *120*, 2449–2456; b) E. L. Merz, V. A. Tikhomirov, I. Krishtalik, *J. Phys. Chem.* **1997**, *101*, 3433–3442.
- [29] Y. Marcus, *J. Solution Chem.* **1984**, *13*, 599–624.
- [30] W. D. Wilson, A. N. Gough, J. J. Doyle, M. W. Davidson, *J. Med. Chem.* **1976**, *19*, 1261–1263.
- [31] A. Molina, J. J. Vaquero, J. L. Garcia-Navio, J. Alvarez-Builla, B. de Pascal-Teresa, F. Gado, M. M. Rodrigo, *J. Org. Chem.* **1999**, *64*, 3907–3915.
- [32] H. Ihmels, S. Leusser, M. Pfeiffer, D. Stalke, *J. Org. Chem.* **1999**, *64*, 5715–5718.
- [33] R. W. Warriner, M. Golic, D. N. Butler, *Tetrahedron Lett.* **1998**, *39*, 4717–4720.
- [34] H. Ihmels, *Eur. J. Org. Chem.* **1999**, 1595–1600.
- [35] I. Fleming, *Frontier Orbitals and Organic Chemical Reactions*, Wiley, New York, **1976**.
- [36] a) M. Klessinger, *Pure Appl. Chem.* **1997**, *69*, 773–778; b) V. Bonacic-Koutecky, J. Koutecky, J. Michl, *Angew. Chem.* **1987**, *99*, 216–236; *Angew. Chem. Int. Ed. Engl.* **1987**, *34*, 170–189.
- [37] M. J. Bearpark, M. Deumal, M. A. Robb, T. Vreven, N. Yamamoto, M. Olivucci, F. Bernardi, *J. Am. Chem. Soc.* **1997**, *119*, 709–718.
- [38] H. G. Viehe, Z. Janousek, R. Merenyi, L. Stella, *Acc. Chem. Res.* **1985**, *18*, 148–154.
- [39] Note: Although the dimers are pure by ¹H NMR spectroscopy and solutions in [D₆]DMSO are stable for weeks, the UV spectra are always contaminated with small quantities of the monomer.
- [40] B. J. Coe, *Chem. Eur. J.* **1999**, *5*, 2464–2471.
- [41] J. N. Demas, G. A. Crosby, *J. Phys. Chem.* **1971**, *75*, 991–1024.
- [42] D. F. Eaton, *Pure Appl. Chem.* **1988**, *60*, 1108–1114.
- [43] M. J. S. Dewar, E. G. Zoebisch, E. F. Healy, J. J. P. Steward, *J. Am. Chem. Soc.* **1985**, *107*, 3902–3909.
- [44] G. Rauhut, A. Alex, J. Chandrasekhar, T. Steinke, W. Sauer, B. Beck, M. Hutter, P. Gedeck, T. Clark, Universität Erlangen, Erlangen, Germany, **1996**.
- [45] B. R. Baker, J. Kozma, *J. Med. Chem.* **1967**, *10*, 682.
- [46] C. K. Bradsher, J. C. Parham, *J. Org. Chem.* **1963**, *28*, 83–85.
- [47] S. Goswami, A. K. Mahapatra, *Tetrahedron Lett.* **1998**, *39*, 1981–1984.

Received: November 2, 1999 [F2113]